AFRL-RW-EG-TR-2013-030

PRACTICAL PHOTONIC BANDGAP CALCULATIONS USING MPB

Douglas V. Nance

AFRL/RWWC
101 W. Eglin Blvd.
STE 334
Eglin AFB, FL 32542-6810

February 2013

INTERIM REPORT

AIR FORCE RESEARCH LABORATORY
MUNITIONS DIRECTORATE

■ **Air Force Materiel Command** ■ **United States Air Force** ■ **Eglin Air Force Base, FL 32542**

NOTICE AND SIGNATURE PAGE

Using Government drawings, specifications, or other data included in this document for any purpose other than Government procurement does not in any obligate the U.S. Government. The fact that the Government formulated or supplied the drawings, specifications, or other data does not license the holder or any other person or corporation, or convey any rights or permission to manufacture, use, or sell any patented invention that may relate to them.

This report was cleared for public release by the 96th Air Base Wing, Public Affairs Office, and is available to the general public, including foreign nationals. Copies may be obtained from the Defense Technical Information Center (DTIC) < http://www.dtic.mil/dtic/index/html>.

AFRL-RW-EG-TR-2013-030 HAS BEEN REVIEWED AND IS APPROVED FOR PUBLICATION IN ACCORDANCE WITH ASSIGNED DISTRIBUTION STATEMENT.

FOR THE DIRECTOR:

Signed	Signed
Craig R. Ewing, DR-IV, PhD	Douglas V. Nance
Technical Advisor	Research Scientist
Weapon Engagement Division	AFRL/RWWC

This report is published in the interest of scientific and technical information exchange, and its publication does not constitute the Government's approval or disapproval of its ideas or findings.

REPORT DOCUMENTATION PAGE

Form Approved
OMB No. 0704-0188

PLEASE DO NOT RETURN YOUR FORM TO THE ABOVE ADDRESS.

1. REPORT DATE *(DD-MM-YYYY)*	2. REPORT TYPE	3. DATES COVERED *(From - To)*
22-02-2013	Interim	1 June 2012 - 30 Sep 2012

4. TITLE AND SUBTITLE

PRACTICAL PHOTONIC BANDGAP CALCULATIONS USING MPB

5a. CONTRACT NUMBER

N/A

5b. GRANT NUMBER

N/A

5c. PROGRAM ELEMENT NUMBER

62602F

6. AUTHOR(S)

Douglas V. Nance

5d. PROJECT NUMBER

2502

5e. TASK NUMBER

67

5f. WORK UNIT NUMBER

63

7. PERFORMING ORGANIZATION NAME(S) AND ADDRESS(ES)

AFRL/RWWC
101 W. Eglin Blvd
Eglin AFB, FL 32542-6810

8. PERFORMING ORGANIZATION REPORT NUMBER

AFRL-RW-EG-TR-2013-030

9. SPONSORING/MONITORING AGENCY NAME(S) AND ADDRESS(ES)

AFRL/RWWI
101 W. Eglin Blvd
Eglin AFB, FL 32542-6810

10. SPONSOR/MONITOR'S ACRONYM(S)

AFRL-RW-EG-TR-

11. SPONSOR/MONITOR'S REPORT NUMBER(S)

AFRL-RW-EG-TR-2013-030

12. DISTRIBUTION/AVAILABILITY STATEMENT

Distribution A. Approved for public release, distribution unlimited. (96ABW-2013-0032)

13. SUPPLEMENTARY NOTES

14. ABSTRACT

This report presents a series of calculations made by using the MIT Photonic Bands computer program to resolve the band structures or dispersion relations associated with a series of 2D and 3D photonic crystal lattices. We emphasis the development of techniques for drafting code input to allow the solution of more complicated crystal lattices that may not be easily described with normal code syntax. Due attention is paid to the minimal surface representation of photonic crystals and how it relates to code expressions drafted using intrinsic code syntax. A validation problem is also solved; the results are compared with archival data for this face-centered cubic crystal.

15. SUBJECT TERMS

Photonic crystal, hermitian, Maxwell equation, dispersion, bandgap

16. SECURITY CLASSIFICATION OF:			17. LIMITATION OF ABSTRACT	18. NUMBER OF PAGES	19a. NAME OF RESPONSIBLE PERSON
a. REPORT	b. ABSTRACT	c. THIS PAGE			Douglas V. Nance
UNCLAS	UNCLAS	UNCLAS	UL	32	19b. TELEPHONE NUMBER *(Include area code)*

Reset

PRACTICAL PHOTONIC BANDGAP CALCULATIONS USING MPB

by

Dr. Douglas V. Nance
AFRL/RWWC
Eglin AFB, FL 32542-6810

TABLE OF CONTENTS

LIST OF FIGURES

SUMMARY

This report presents a series of calculations made by using the MIT Photonic Bands computer program to resolve the band structures or dispersion relations associated with a series of 2D and 3D photonic crystal lattices. We emphasize the development of techniques for drafting code input to allow the solution of more complicated crystal lattices that may not be easily described with normal code syntax. Due attention is paid to the minimal surface representation of photonic crystals and how it relates to code expressions drafted using intrinsic code syntax. A validation problem is also solved; the results are compared with archival data for this face-centered cubic crystal.

1.0 INTRODUCTION

This technical report is intended to present the results for a series of practical, computational problems for the MIT Photonic Bands (MPB) computer program. MPB is designed to solve Maxwell's equations for electromagnetic wave propagation in photonic crystals. MPB solves this system of vector equations as a Hermitian eigenproblem using the plane wave approximation.[1,2] In its standard mode of operation, MPB calculates dispersion relations for a chosen photonic crystal. A dispersion relation is a function of the form $\omega = \omega(\vec{k})$, where ω is the angular frequency for the light wave and $\vec{k}$ is the wave vector. The locus of $\vec{k}$ is delineated by the irreducible Brillouin zone (IBZ) for the unit cell of the lattice for the photonic crystal.[2] A dispersion relation can be computed for each "band" of electromagnetic (E/M) propagation. The term band, in this case, is synonymous with the concept of a "mode" of structural vibration. It is effectively a stationary shape for the electromagnetic wave defined in the particular band. Also, each band is generally confined to a specific, finite interval of frequencies, e.g., [ω_1 , ω_2] for the entire range of wave vectors designated for the IBZ.[2]

MPB is a computer program that is widely used by the scientific community. It performs very well in the computation of photonic bands. Yet, MPB does require that its user acquire a significant amount of skill, especially when setting up problems that depart from the examples provided in the documentation. A principle reason for the learning curve is that MPB uses a flexible scripting language called "Scheme" for its input files.[4] For legacy programmers who have teethed on compilers like FORTRAN and C, Scheme is an acquired taste. This fact stands as partial motivation for the creation of this report. Rather than a compiler-based structure, Scheme relies upon an interpreter. There are many such interpreters, but MPB (and the CTL control language) rely upon GNU Guile, a powerful UNIX-based Scheme interpreter.[5]

Photonic crystals are comprised of periodic distributions of dielectric material. In order to solve for the band structure of a chosen crystal, the spatial distribution of dielectric material must be input into MPB as must its lattice description. The lattice description takes the form of a set of basis vectors; the lengths of these vectors are based upon a lattice constant, the fundamental unit of distance on the crystal lattice.[6] These items are easily input into MPB by using Scheme or CTL (MPB-specific additions to Scheme) syntax. The spatial distribution of dielectric material can be more complicated to code. Simple geometric figures such as circles, cylinders, rectangular boxes and ellipsoids can be easily described by intrinsic Scheme syntax already programmed into MPB.[6] If a geometry is not represented by an intrinsic function, it can be much more difficult to program into MPB. A means for accomplishing this task is also a subject of this report. In particular, we address the representation of a so-called minimal surface in MPB. More importantly, we show that our description of the minimal surface is correct and produces the correct dispersion relation.

A final issue of interest is the validation of MPB for photonic crystals of interest. We do not question the fact that MPB is completely validated, i.e., that it produces the correct physical output for a properly described photonic crystal. Yet, it is important to see that MPB, when operated by the novice user, produces the correct output for specific photonic crystals. In this case, we choose a photonic crystal of particular interest to us; compute the dispersion relation, and compare MPB's results to those in the archival literature.

This report is organized as follows. Section 2 provides detailed descriptions of the test problems we have selected for bandgap analysis. A significant amount of attention is paid to the crystal lattice configurations and to the geometric distributions of dielectric material. We also discuss the relationship between the MPB's intrinsic syntactical descriptions of geometry and the interpretation of geometry via minimal surfaces. Section3 presents the results of our MPB analyses along with attendant band structure comparisons as proof of the validity of our modeling approach. Basic conclusions emerging from this work are discussed in Section 4 along with comments regarding the future usability of MPB for our continuing study of photonic crystals.

2.0 METHODS, ASSUMPTIONS AND PROCEDURES

In order to determine the dispersion relations or band diagrams for a photonic crystal, a Hermitian eigenproblem must be solved by numerical methods. Given that this problem and the algorithms used to solve it are thoroughly documented elsewhere, these discussions are omitted from this report. Interested readers are referred to References 2, 3 and 7. Rather than a presentation of theory, this section describes the photonic crystal configurations that we find interesting. Moreover, we include many details on the distribution of dielectric material for each crystal with a lot of emphasis on how it is represented in MPB.

2.1 The 2D Offset Square Dielectric Vein Lattice

In our early investigations of photonic bandgaps, we examined the 2D square dielectric vein lattice.[7] This lattice is described by the two orthogonal vectors in the *x* and *y* Cartesian directions. This lattice renders a simple checkerboard pattern as illustrated in Figure 1. The veins in the lattice are made of dielectric material while air fills the square voids in the lattice. We have noted that while band gaps are observed for high contrast dielectric ratios, no gaps are observed for low contrasts say, for dielectrics such as chitin. General curiosity motivates us to examine a similar lattice where the "rows" of air cells are offset from one another rendering a "brick-like" pattern as is shown in Figure 2. Here, the lattice vectors are oblique and non-orthogonal; in fact, they may be written as

$$\begin{aligned} \vec{a}_1 &= (1, 0)^T \\ \vec{a}_2 &= (\beta, 1)^T \end{aligned} \tag{1}$$

The reciprocal lattice vectors are

$$\begin{aligned} \vec{b}_1 &= 2\pi(1, -\beta) \\ \vec{b}_2 &= 2\pi(0, 1) \end{aligned} \tag{2}$$

For our purposes, the parameter β is chosen such that $0 < \beta < 1$.

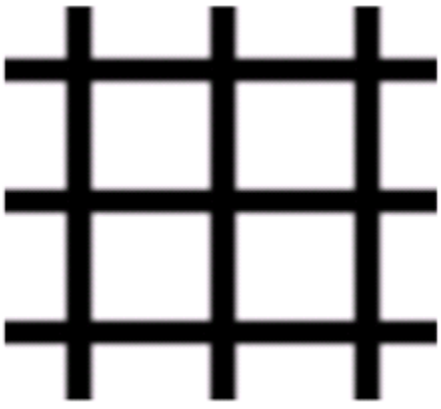

Figure 1. The square dielectric vein lattice. Dark lines indicate dielectric material; the white voids contain air

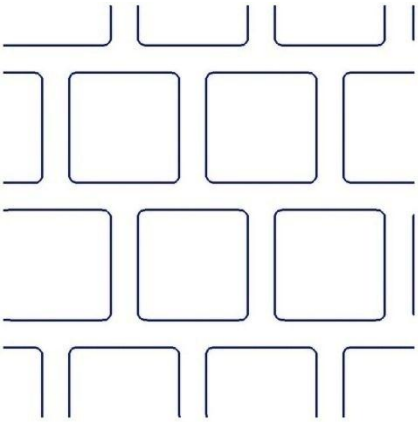

Figure 2. The square brick dielectric vein lattice; square regions are filled with air; the remainder of the lattice is filled with dielectric material

For the brick lattice, the width of a dielectric vein is designated as $0.2a$, where a is the lattice constant. As is shown in Figure 2, this lattice is offset by half the width of one square air cell; this case corresponds to a β value of ½. Accordingly, the Brillouin zone (BZ) can be graphed as is shown in Figure 3; plot 3(a) is for β = ½ while 3(b) is for the case where $\beta = \frac{1}{3}$.[8] To complete the description of this lattice, symmetry points are labeled around the irreducible Brillouin zone (IBZ) for these lattices.[3] We have attempted to conform to the labeling convention when possible. In this report, we compute dispersion relations for β equal to ½, $\frac{1}{3}$ and ¾. For the case where β = ¾, the BZ has the shape of a left/right mirror image of Figure 3(b), so its graph is omitted from this report. Note that we use the term "offset" in the caption of Figure 3. This term refers to brick lattices that do not have vein attachments at the air cell midpoints (when $\beta \neq$ ½).

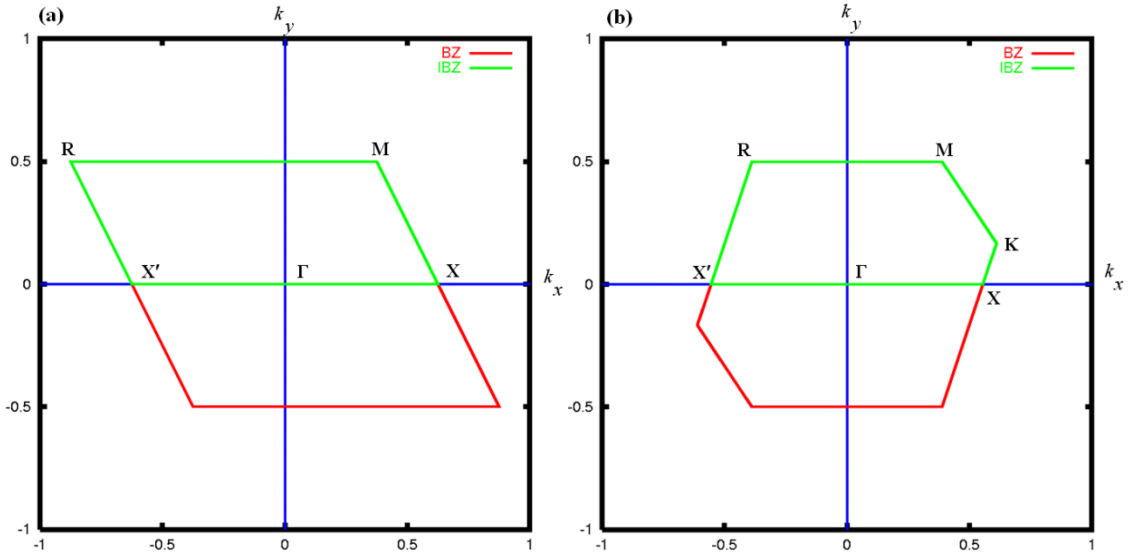

Figure 3. Brillouin zones (BZ) for offset square vein dielectric lattices. (a) for β = ½ (b) for $\beta = \frac{1}{3}$. Points of high symmetry are labeled around the irreducible Brillouin zone (IBZ)

2.2 The Diamond Minimal Surface

The diamond crystal lattice is a well established test case for MPB. In this case, we have a set of dielectric spheres, oriented in the diamond configuration, immersed in air. Naturally, these spheres form a surface in a supercell. We may use a minimal surface to represent the collective surface for the dielectric spheres.[9] The equation for the minimal diamond surface is

$$\cos(Z)\sin(X+Y)+\sin(Z)\cos(X-Y)=t \tag{3}$$

where

$$X=\frac{2\pi x}{a};\quad Y=\frac{2\pi y}{a};\quad Z=\frac{2\pi z}{a},\qquad 0\le x,y,z\le 1$$

For this configuration, the unit cube contains the supercell. The distribution of dielectric material in the supercell is given by the use of (3), albeit in a slightly different form, i.e., let

$$f(X,Y,Z)=\cos(Z)\sin(X+Y)+\sin(Z)\cos(X-Y) \tag{4}$$

Then the dielectric permittivity is set according to the formula

$$\varepsilon=\begin{cases}\varepsilon_{dielectric}, & f(X,Y,Z)\le t\\ \varepsilon_{air}, & f(X,Y,Z)>t\end{cases} \tag{5}$$

The parameter t controls the volume fraction of dielectric material in the supercell. The relationship between dielectric volume fraction and t is shown in Figure 4. A direct comparison can be made between the diamond configurations as described by discrete spheres (MPB intrinsic syntax) and by the minimal surface description (equations 3 through 5) if we note that

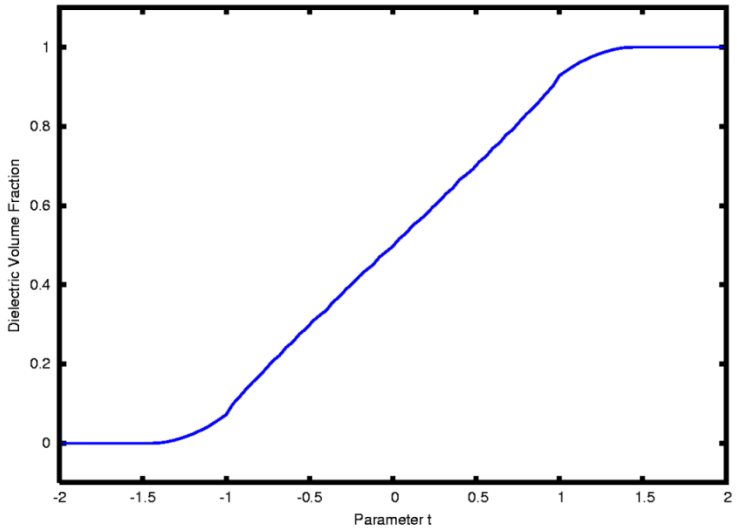

Figure 4. Plot of dielectric volume fraction versus minimal surface parameter *t* for the diamond configuration

there is a relationship between dielectric volume fraction for the minimal surface and the radius of the discrete dielectric spheres. This relationship is shown in Figure 5. On this basis, we can plot iso-surface contours of the dielectric function for both the discrete spheres (MPB intrinsic syntax) and for the minimal surface. These plots are shown in Figure 6 for the dielectric volume fraction of 0.19.

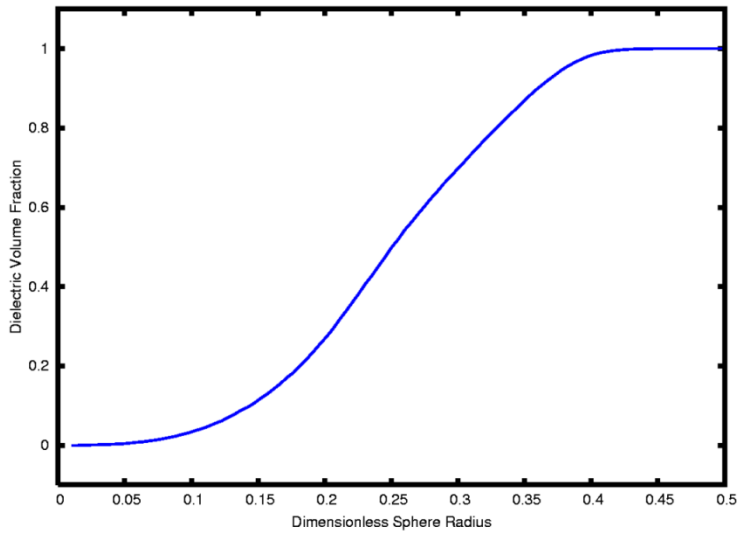

Figure 5. Plot of dielectric volume fraction versus the discrete spherical radius for the diamond configuration

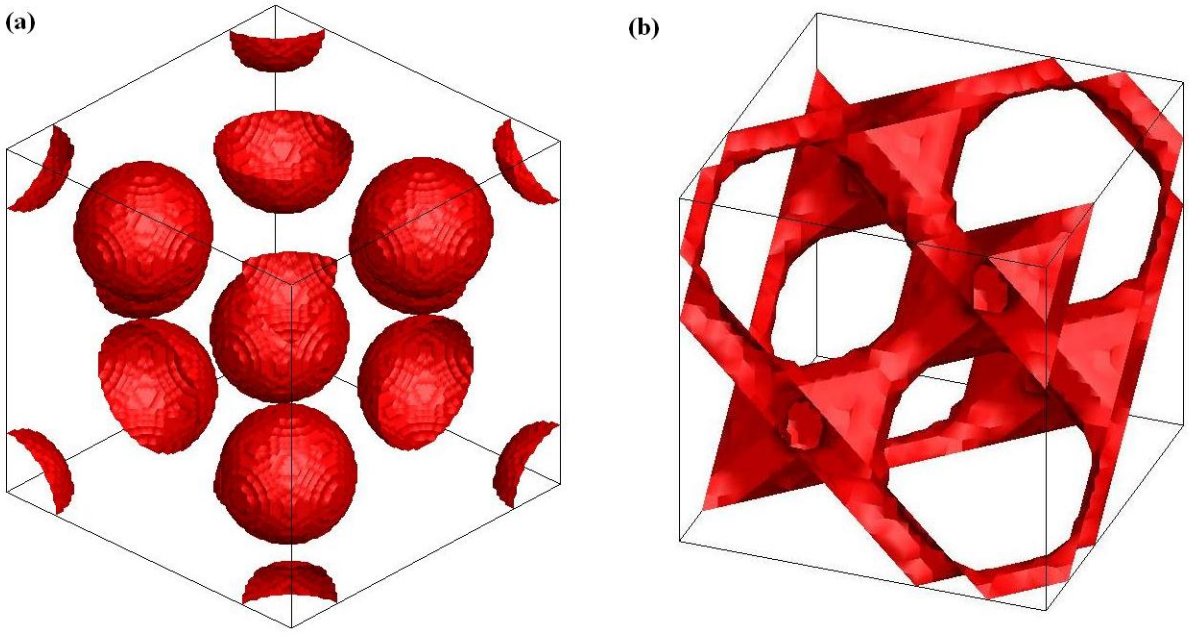

Figure 6. Iso-surface plots of dielectric permittivity (based upon equations) for (a) the discrete sphere model and (b) for the minimal surface model of the diamond configuration with 19% volume fraction

Both of the plots shown in Figure 6 are generated by programming equations for the dielectric distributions and graphing the resulting data. Recall that we know the equations and

point locations for the spheres in the discrete model. Obviously, equations 3 through 5 are used for the minimal surface plot. Comparing Figures 6a and 6b is not an easy task since (i) the minimal surface is continuous, unlike the discrete model, and (ii) the post-processor contours differently around the void regions. In any case, the triangular orientation of the dielectric spheres is reflected. In 6b, the spheres exist at the red clusters in between the white voids. One can also see dielectric material representing neighboring spheres at the supercell corners. An interesting and important fact is that the minimal surface represents a fully connected dielectric field unlike the discrete model. Figure 7 contains plots of the same dielectric field, but in this case, the plots are generated by post-processing the dielectric field generated by MPB. Just as is indicated by Figure 6, the minimal surface model captures the tetrahedral distribution of the

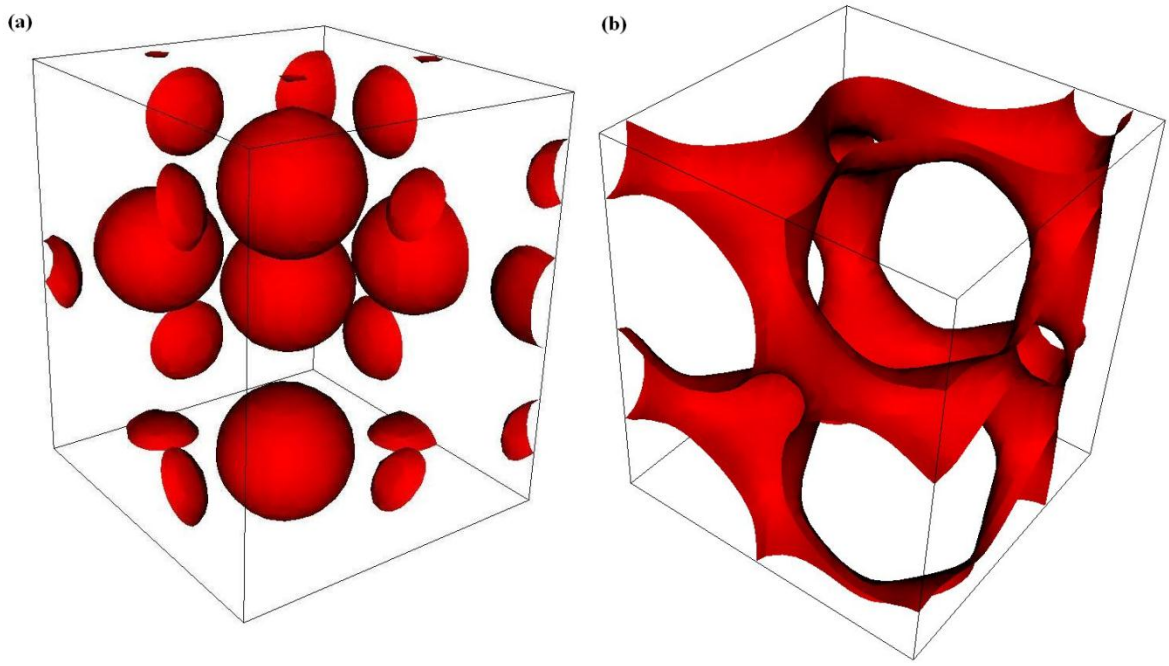

Figure 7. Plots of the dielectric field generated by MPB for (a) the discrete model and (b) the minimal surface model for the diamond configuration at volume fraction 19%

dielectric spheres. Again, we see that the minimal surface represents a fully connected distribution of dielectric material. We show these comparisons because the minimal surface must be explicitly coded into MPB's control (or input) files without the benefit of intrinsic surface description syntax. In fact, the minimal surface must be described by writing code in the Scheme programming language. By using the information contained in Figures 4 and 5, we can develop the dielectric material distribution for a dielectric volume fraction of 30%. This distribution is shown in Figure 8. Although it is difficult to see, the minimal surface representation does capture the proper distribution of dielectric material. The underlying tetrahedral configuration is visible. This behavior is echoed by Figure 9, plots for the same dielectric distribution generated by MPB (and its subsystems). The use of programmed minimal surfaces (or other non-intrinsic geometries) is very important for future applications of MPB. Scheme programming segments can be written to describe complex geometries that cannot be scripted in MPB control input syntax. A possible example of this idea is the gyroid lattice.[10] A minimal surface equation exists for the gyroid, but a means for representing the gyroid in terms of MPB intrinsic syntax is

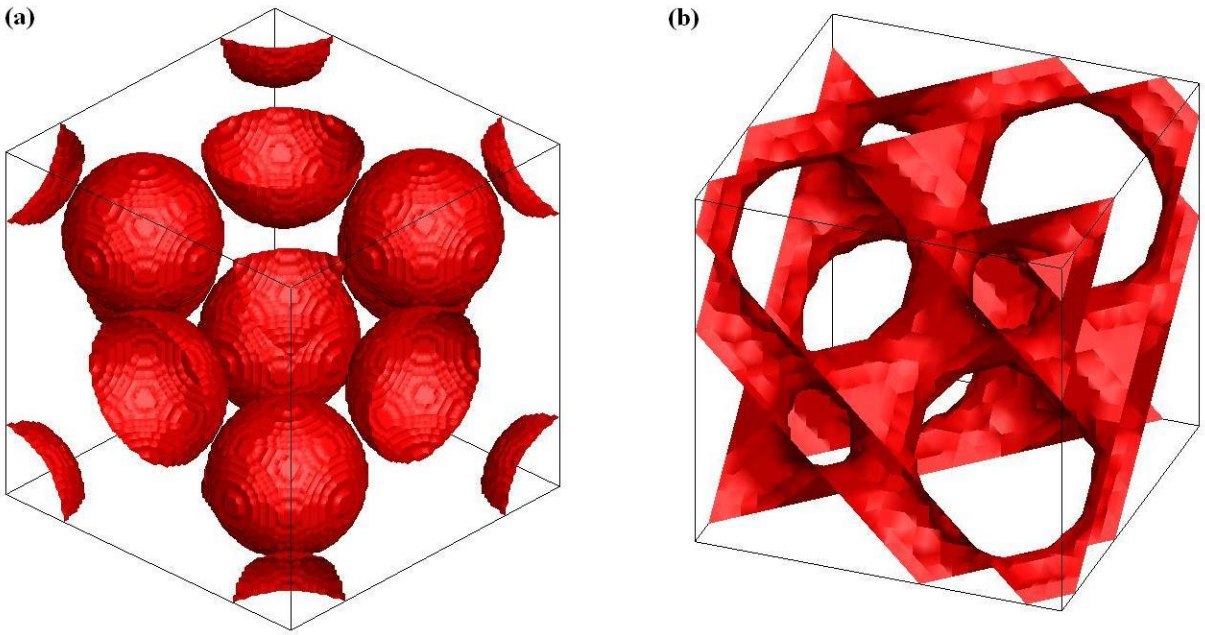

Figure 8. Iso-surface plots of dielectric permittivity (based upon equations) for (a) the discrete sphere model and (b) for the minimal surface model of the diamond configuration with 30% volume fraction

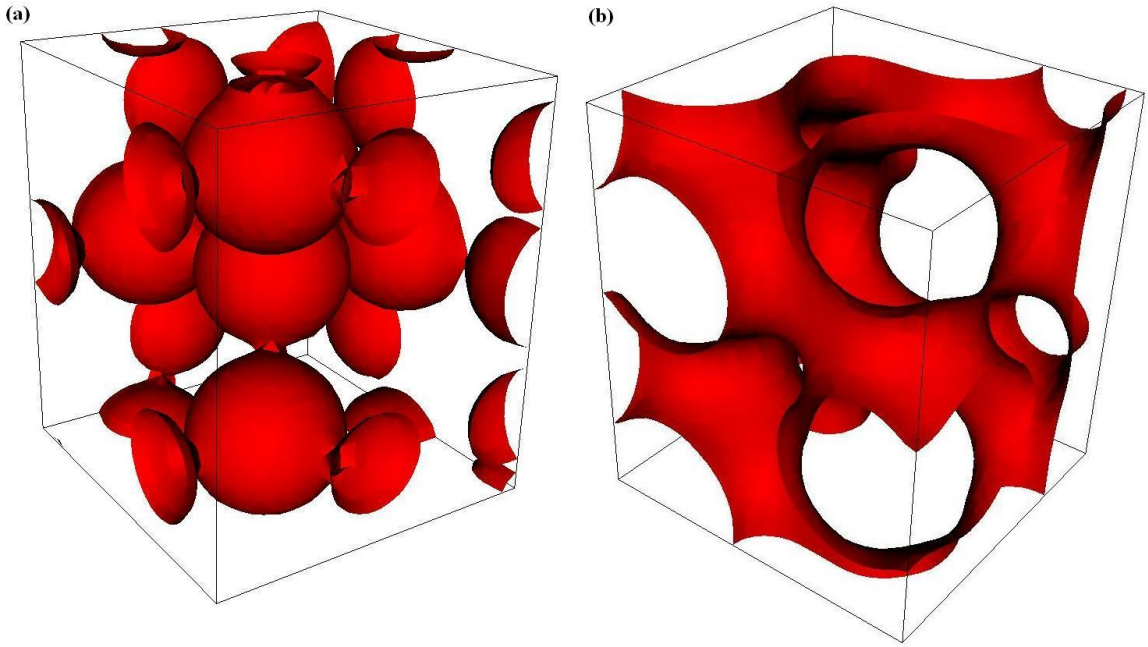

Figure 9. Plots of the dielectric field generated by MPB for (a) the discrete model and (b) the minimal surface model for the diamond configuration at volume fraction 30%

not currently clear.[11,12] Dispersion relations are computed for both the discrete and minimal surface diamond configurations discussed above. Results for these configurations are presented and discussed in Section 3.

2.3 Example of a Biological Photonic Crystal

A final thrust of this report is to validate, in some sense, the accuracy of an MPB solution for a real-world photonic crystal. Many such crystals can be found in nature, particularly in the exoskeletons of insects. One crystal that is well documented in the scientific literature comes from *Lamprocyphus augustus*, a green weevil known for its brilliant coloration.[13,14,15] This crystal is a relatively simple arrangement of dielectric and air on the face-centered cubic (FCC) lattice. An air cylinder is placed at each lattice point in a dielectric field; the axis of each cylinder axis is aligned along the direction $\hat{i}+\hat{j}+\hat{k}$ (111). In this lattice, the cylinders take on a staggered appearance with an overall hexagonal distribution in the lateral directions. This 3D crystal is arranged with layers of dielectric rods alternating with layers of cylindrical air voids.[16] The radius and length of cylinder are given as 0.27 and 0.89, respectively, while the lattice constant is set at unity. The background dielectric material has a relative permittivity of 5.29. The orientation of the air cylinders in the dielectric takes on the appearance shown in Figure 10.

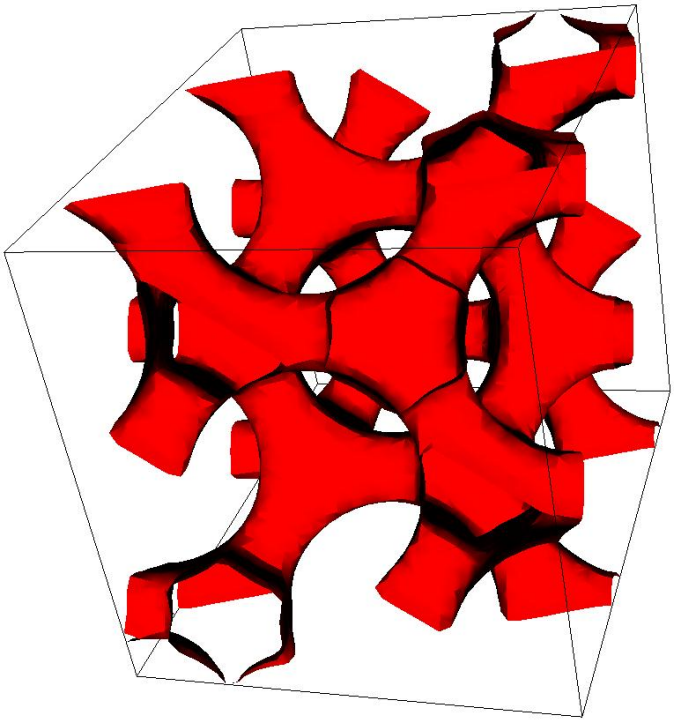

Figure 10. An iso-surface plot of dielectric permittivity for the 3D layered crystal consisting of cylindrical voids of air suspended in a background dielectric structure. The air cylinders are aligned with the vector $\hat{i}+\hat{j}+\hat{k}$, i.e., direction (111)

The dispersion relation computed for this crystal can be compared with an archived dispersion relation.[15] A satisfactory comparison of these relations provides good evidence that MPB is a useful tool for computing the band structure and electromagnetic wave modes for biological crystals.

3.0 RESULTS

In this section, we present the results of dispersion relation (or photonic band) calculations for the test problems described in the preceding section. Since our objective is to prove sound our skills for setting up MPB problems, we concentrate exclusively on band calculations. Neither electric nor magnetic field shapes are shown here.

3.1 Band Structure for the 2D Square Brick Dielectric Vein Lattice

To evaluate the effect of the geometric offset of the square "brick" lattice, dispersion relations are computed for β equal to ⅓, ½ and ¾ for a dielectric permittivity value of 2.31. These relations are plotted in Figures 11 through 13, respectively. It is interesting to observe that a narrow band gap (5.58 %) exists only for β equal ½. This fact is very interesting because the

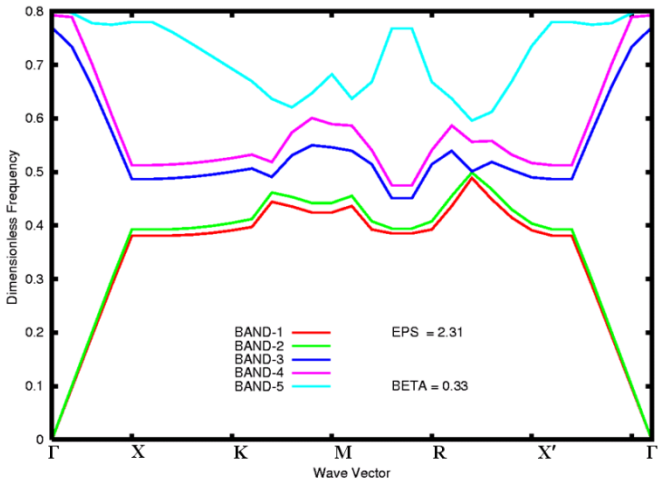

Figure 11. Dispersion relation for the dielectric vein square brick dielectric vein lattice with $\beta = \frac{1}{3}$

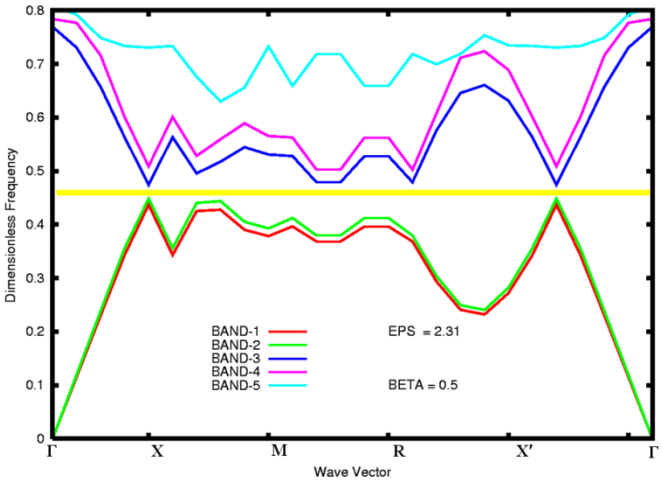

Figure 12. Dispersion relation for the square brick dielectric vein lattice with $\beta = ½$. The yellow bar indicates the presence of a bandgap

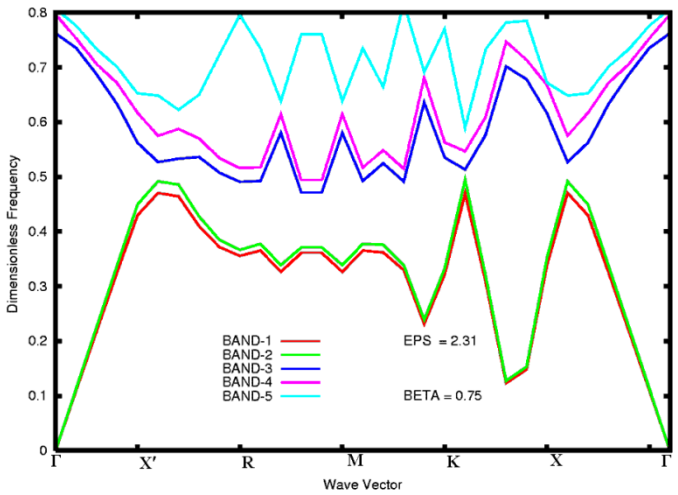

Figure 13. Dispersion relation for the dielectric vein square brick lattice with β = 3/4

square dielectric lattice with zero offset exhibits absolutely no band gaps for this value of the dielectric permittivity.[7] It seems that vein connections existing at the midpoint of the square cell are sufficient to force the electromagnetic field into a lower frequency range creating a band gap. This result was not anticipated. It does pique the interest and motivate the following question. Is there an optimal value of dielectric permittivity for this 2D photonic crystal? This question is easily answered with a little numerical effort. Consider the plot shown in Figure 14. It is evident that the band gap width varies smoothly over the range of dielectric permittivity

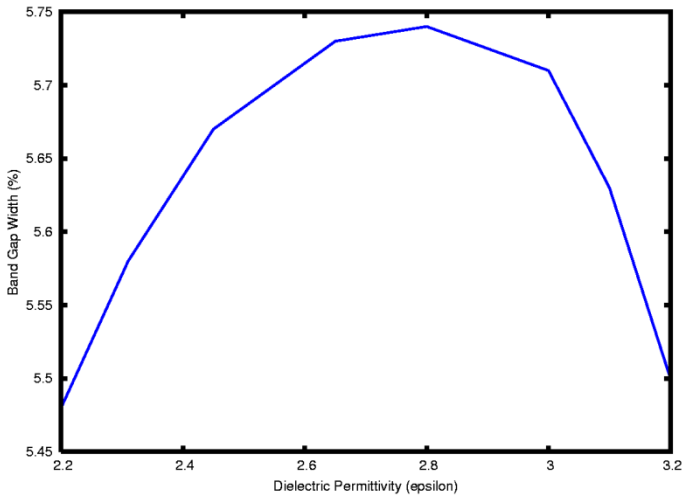

Figure 14. Plot of percent band gap width versus dielectric permittivity resulting from a parametric study conducted for the offset square brick lattice with β = 0.5

values, but the gap width peaks at 5.74% for ε = 2.8. The dispersion relation looks virtually identical to that shown in Figure 12, so a plot for β = 0.5, ε = 2.8 is omitted from this report. This band gap result is worthy of some consideration. A common practice is to build 3D photonic crystals from stacks of 2D crystals. In some cases, this technique may provide an easier method of fabrication for certain 3D photonic crystals.[16]

3.2 Band Structure for the Diamond Minimal Surface

The goal of this section is to show that we can utilize the minimal surface description of a photonic crystal in lieu of the discrete geometric description (should the latter even exist). In the interest of practicality, we have selected the diamond photonic crystal (see Figures 6 through 9) in the preceding section) as a testbed for this idea. As a brief review, the diamond structure is built upon the face-centered cubic (FCC) crystal lattice, and the Brillouin Zone (BZ) is a truncated octahedron.[3,17,18] See Appendix I for a brief discussion of this BZ. The methodology for this study is simple. We compute dispersion relations for both the discrete and minimal surface descriptions and compare them on a band per band basis. A band in this case is a particular relationship of the form $\omega = \omega(\vec{k})$ where ω is angular frequency (or its dimensionless analog), and $\vec{k}$ represents the locus of wave vectors (also dimensionless) around the IBZ. The bands are ordered in some sense, i.e., the frequencies are (on the average) lower for band 1 than for band 2, lower for band 2 than for band 3, and so forth. This behavior is reflective of what is observed in Figure 11 through 13, albeit for a different photonic crystal. Consider the first band for a diamond photonic crystal with a dielectric volume fraction of 0.19 as is shown in Figure 15. Note that a volume fraction of 0.19 corresponds to a radius of 0.178551a and a

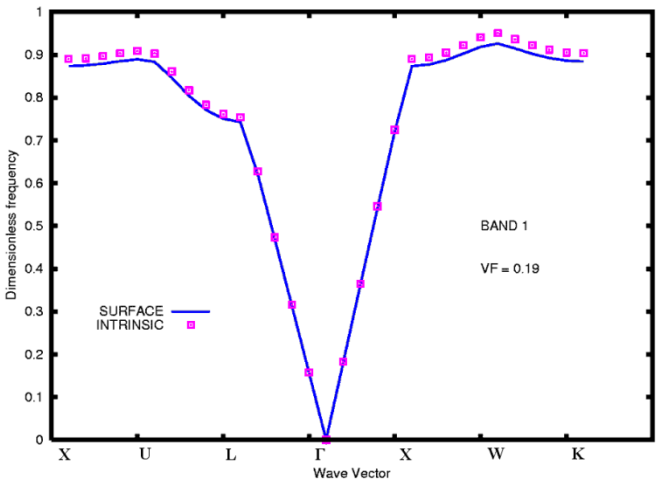

Figure 15. Dispersion relations for the diamond crystal structure with volume fraction 0.19 for both minimal surface and intrinsic MPB syntax descriptions of the first band

minimal surface parameter t = -0.756639. The blue line represents the minimal surface while discrete points are plotted for the intrinsic syntax description. It is evident that the two dispersion relations compare favorably. Consider Figure 16, dispersion relation graphs for the second band computed at the same volume fraction. Again, the comparison is quite favorable. As an additional check, we have computed the third band (the next higher frequency locus) and produced Figure 17. The outcome is no different; the dispersion relations computed by using the diamond minimal surface and MPB's intrinsic geometries are nearly the same. Our examination of the supercell geometries shown in the preceding section tends to indicate that the small difference observed between the dispersion relations may be due to the fact that the dielectric

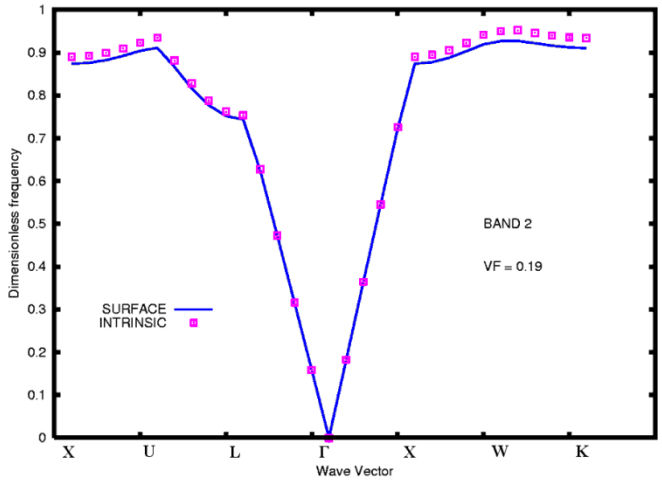

Figure 16. Dispersion relations for the diamond crystal structure with volume fraction 0.19 for both minimal surface and intrinsic MPB syntax descriptions of the second band

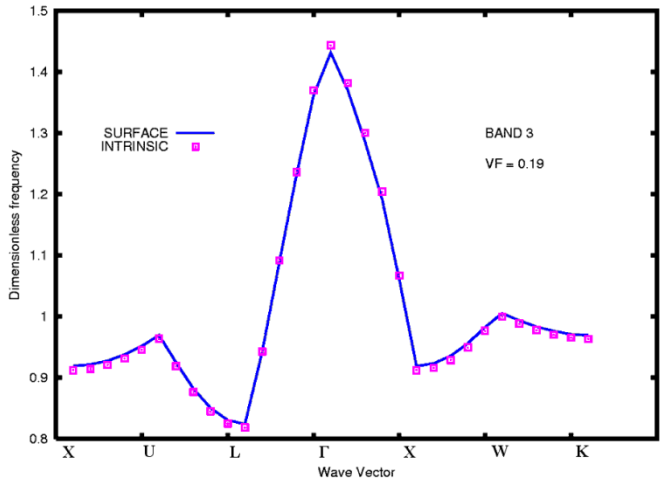

Figure 17. Dispersion relations for the diamond crystal structure with volume fraction 0.19 for both minimal surface and intrinsic MPB syntax descriptions of the third band

structure for the minimal surface is fully connected throughout the lattice. Of course, the discrete (intrinsic MPB syntax) geometric dielectric structure is not connected (due to its use of discrete spherical masses of dielectric material). This fact may force the minimal surface band onto a slightly lower frequency locus along the outer periphery of the IBZ. It is worthwhile to verify this behavior for a configuration involving a higher dielectric volume fraction. Figures 18 through 20 contain plots of the dispersion relations for bands 1 through 3, respectively, for a volume fraction of 0.30. This volume fraction corresponds to a dielectric sphere radius of 0.207599a and a minimal surface parameter t = -0.5. As is evidenced by these plots, there is a favorable comparison between the two solutions for each band. On the whole, the difference between the two solutions decreases as the order of the band increases. This behavior seems reasonable since longer electromagnetic waves are more likely to sense the difference in the dielectric distribution for the crystal. That is to say, the concentrated regions of dielectric material are slightly smaller for the minimal surface model than for the discrete spheres model.

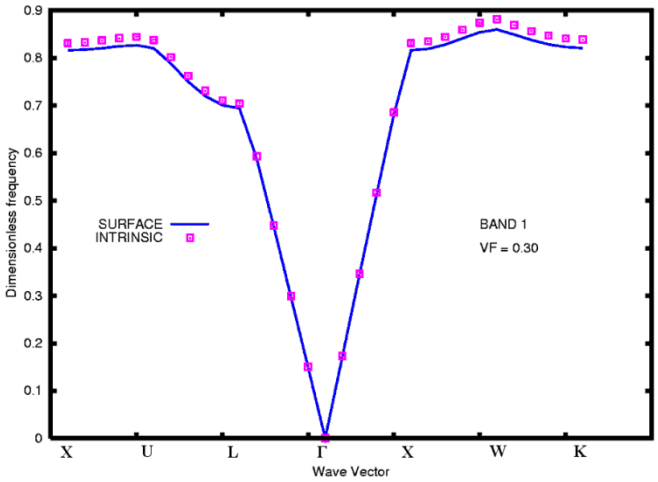

Figure 18. Dispersion relations for the diamond crystal structure with volume fraction 0.30 for both minimal surface and intrinsic MPB syntax descriptions of the first band

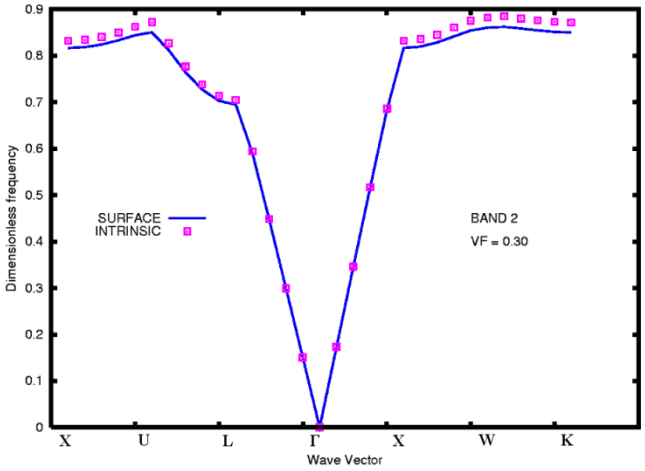

Figure 19. Dispersion relations for the diamond crystal structure with volume fraction 0.30 for both minimal surface and intrinsic MPB syntax descriptions of the second band

For the minimal surface model, this characteristic provides connectivity everywhere while preserving the dielectric volume fraction. A long wavelength electromagnetic field cannot as effectively concentrate its energy effectively in these smaller dielectric volumes. Hence, we observe larger differences between bands existing at lower frequencies.

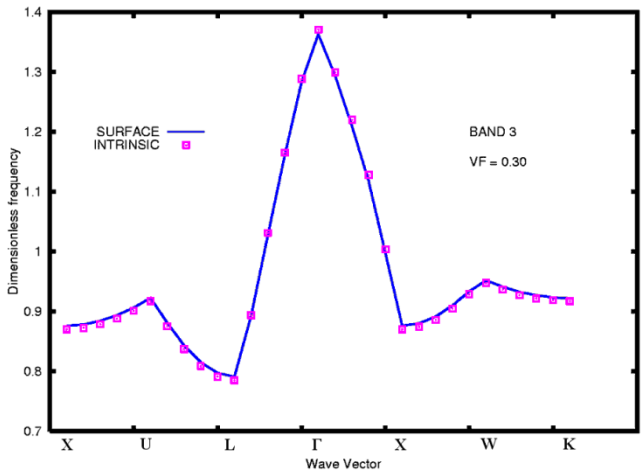

Figure 20. Dispersion relations for the diamond crystal structure with volume fraction 0.30 for both minimal surface and intrinsic MPB syntax descriptions of the third band

3.3 Band Structure for the Biological Photonic Crystal

The results in this section confirm that MPB is suitable for computing the band structure for biological photonic crystals. The only caveat for this claim is that a user must be capable of correctly coding the crystal structure for MPB input. In this case, we have used MPB to determine the band structure for the stacked (or layered) dielectric rod and air-cylinder 3D

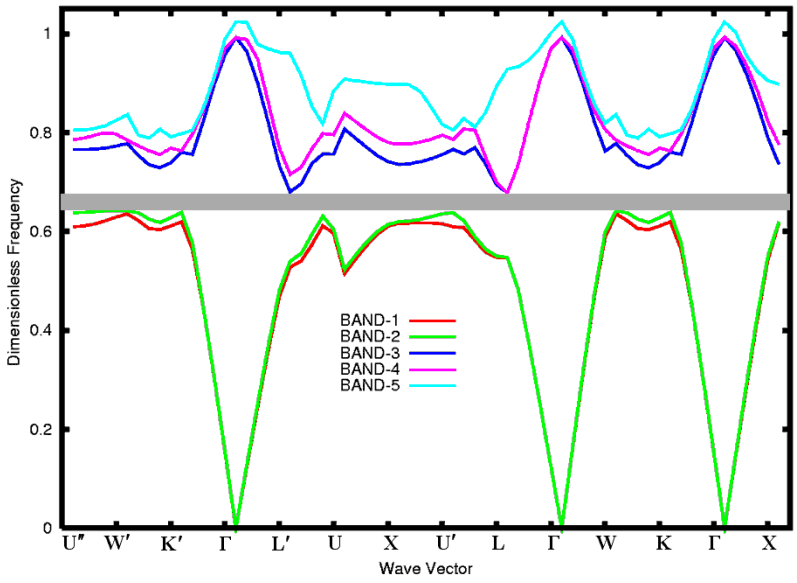

Figure 21. Dispersion relation for the layered photonic crystal consisting of air cylinders suspended in a dielectric material with relative permittivity of 5.29

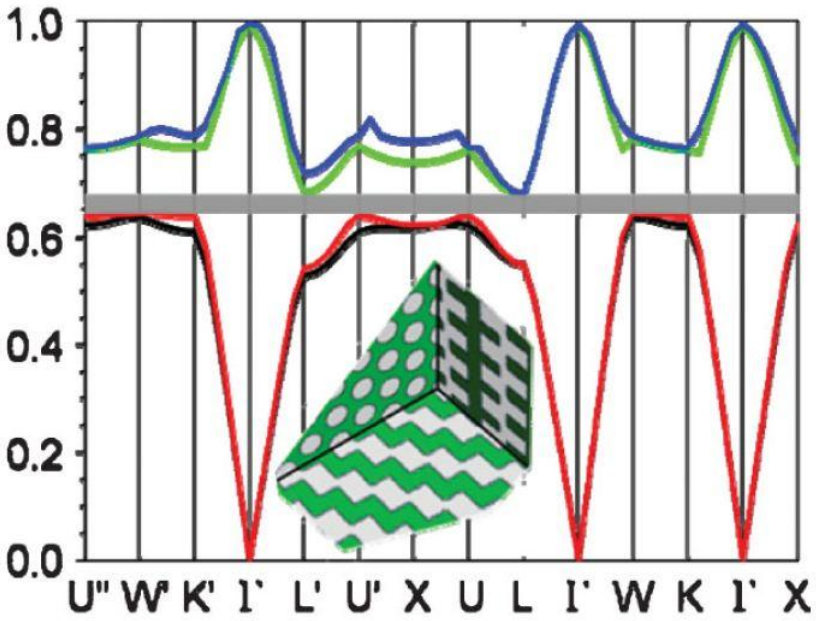

Figure 22. Dispersion relation for the layered photonic crystal reprinted from Reference [15]

photonic crystal described in Section 2.3. The first five bands are calculated for a resolution value of 32 pixels. The computed band structure (dispersion relation) is shown in Figure 21. As you can see, this configuration has a small photonic band gap (between bands 2 and 3) indicated by the lengthy gray box drawn on the front of the graph. The band gap width computed by MPB is 5.39%. The referenced source reports a width of 5% for the gap existing between bands 2 and 3.[15] This data indicates good agreement between the solutions. The major difference between the two solutions is that our band structure predicts a sharp reduction in frequency for bands 1 and 2 near the symmetry point we designate as "U" (symmetry point U' in [15]). It follows that a truly exact comparison is difficult to make since we have neither the author's data tables nor the actual BZ symmetry point listing used in the reference. To aid in making a visual comparison, the archived dispersion relation is shown in Figure 22. Again, the agreement is quite good up to the detailed arrangement of symmetry points. Both the Cartesian coordinates of the symmetry points as well as the resolution of the archived results are unknown.

4.0 CONCLUSIONS

This report has presented results for a series of practical bandgap calculations made by using the MIT Photonic Bands (MPB) electromagnetic wave solver. Dispersion relations have been calculated for a series of 2D and 3D photonic crystals. The two-dimensional crystal addressed is the square brick dielectric vein lattice. Related to the standard square dielectric vein lattice, the brick configuration has oblique lattice vectors spanning an acute angle instead of the right angle used for the standard case. For lattice vectors spanning 45˚, the brick lattice has a 5% bandgap for a relative permittivity of 2.31. This result presents a stark contrast to the standard case that has no band gap in this permittivity range. The brick lattice may be worthy of consideration for the creation of stacked 3D photonic crystals.

The second test problem addressed by the report surrounds testing different types of input for the diamond crystal lattice. This lattice is commonly analyzed by MPB through the use of its intrinsic syntax. That is to say, MPB syntax can be used to describe a diamond lattice composed of spherical masses of dielectric material (or the associated inverse lattice). However, coding more complicated distributions of dielectric material is a matter of concern. It may not be possible to describe other crystals of interest in terms of simple geometric shapes. For this reason, we have carefully coded the diamond lattice in the form of minimal surface equations. As it happens, we can describe a wide array of crystal lattices in mathematical form. Complicated dielectric functions can be entered into MPB by bypassing MPB's intrinsic syntax and coding the description in the "Scheme" programming language, the interpreter that MPB input is based upon. We have accomplished this for the diamond lattice using both the intrinsic syntax and the minimal surface input. The band structures obtained show very good agreement with one another, and we have proved an important concept. We can code dielectric structures directly into MPB as long as we can obtain a mathematical description for the distribution of dielectric material.

In the way of code validation, we have solved for the band structure associated with a 3D photonic crystal of interest. We have coded the face-centered cubic crystal structure for an exoskeletal scale from *Lamprocyphus augustus*, a green weevil, into MPB and extracted its band structure for an expanded Brillouin Zone. This result is compared with the archived band structure accepted by the scientific community. Our prediction shows very good agreement with the accepted dispersion relation. This is not surprising since MPB is essentially the academic standard tool for the calculation of photonic bandgaps. We have significant confidence in MPB's abilities, but there is a noticeable learning curve associated with its use. Educating the user in building MPB input and in interpreting MPB output is a task of significance mass. The exercises described here have provided us with reasonable confidence in applying MPB to study photonic crystals of greater complexity.

The lack of experimental photonic bandgap data is worthy of comment. To date, no references containing experimentally obtained photonic bandgap plots have been found. One empirically inferred bandgap has been located, but the associated plot is really cast in terms of reflectivity.[13] Hence, this result is not a dispersion relation. Further investigation has shown that the authors of this reference actually used MPB in order to obtain their dispersion relation. There are procedures existing in the archival literature for the experimental measurement

(perhaps through indirect means) of dispersion relations (or band structures) for photonic crystals.[20] It is hoped that through the implementation of these procedures or through new methods we will soon be able to experimentally determine photonic band structures.

REFERENCES

1. Sözüer, H.S. and Haus, J.W., "Photonic bands: simple-cubic lattice", *J. opt. Soc. Am. B*, Vol. 10, No. 2, pp. 296-302, 1993.

2. Johnson, S.G. and Joannopoulos, J.D., "Block-iterative frequency-domain methods for Maxwell's equations in a planewave basis", *Optics Express*, Vol. 8, No. 3, 2001.

3. Joannopoulos, J.D., Johnson, S.G., Winn, J.N. and Meade, R.D., *Photonic Crystals: Molding the Flow of Light*, 2nd Ed., Princeton University Press, Princeton, NJ, 2008.

4. Johnson, S.G., "LIBCTL Ver. 3.1 User Manual", http://ab-intio.mit.edu/wiki/index.php/ Libctl_manual.

5. "GNU Guile 1.8 Reference Manual", http://www.gnu.org/software/guile/docs/docs.html.

6. Johnson, S.G., "MPB ver. 1.4.2 User Reference Manual", ", http://ab-intio.mit.edu/wiki/ index.php/MPB_User_Reference.

7. Nance, D.V., "A Comparison of the Performance of 2D Square and Rectangular Dielectric Vein Structures", Technical Report AFRL-RW-EG-TR-2012-114, 2012.

8. Cunningham, S.L., "Special points in the two-dimensional Brillouin zone", *Physical Review B*, Vol. 10, No. 12, pp. 4988-4994, 1974.

9. Michielsen, K. and Kole, J.S., "Photonic band gaps in materials with triply periodic surfaces and related tubular structures", *Physical Review B*, Vol. 68, 115107, pp. 1-13, 2003.

10. Wohlgemuth, M., Yufa, N., Hoffman, J. and Thomas, E.L., "Triply periodic bicontinuous cubic microdomain morphologies by symmetries", *Macomolecules*, Vol. 34, pp. 6083-6089, 2001.

11. Poladian, L., Wickham, S., Lee, K., Large, M.C.J., "Iridescence from photonic crystals and its suppression in butterfly scales", *J. R. Soc. Interface*, Vol. 6, pp. S233-S242, 2009.

12. Grosse-Brauckmann, K., "On gyroid interfaces", *Journal of Colloid and Interface Science*, Vol. 187, pp. 418-428, 1997.

13. Wilts, B.D., Michielsen, K., De Raedt, H. and Stavenga, D.G., "Hemispherical Brillouin zone imaging of a diamond-type biological photonic crystal", *J. R. Soc. Interface*, doi: 10.1098/ rsif.2011.0730, 2011.

14. Galusha, J.W., Richey, L.R., Gardner, J.S., Cha, J.N. and Bartl, M.H., "Discovery of a diamond-based photonic crystal structure in beetle scales", *Physical Review E*, Vol. 77, 050904, pp. 1-4, 2008.

15. Galusha, J.W., Jorgensen, M.R. and Bartl, M.H., "Diamond-structured titania photonic-bandgap crystals from biological templates", *Adv. Materials*, Vol. 22, pp. 107-110, 2010.

16. Johnson, S.G. and Joannopoulos, J.D., "Three-dimensionally periodic dielectric layered structure with omnidirectional photonic band gap", *Applied Physics Letters*, Vol. 77, No. 22, pp. 3490-3492, 2000.

17. Bradley, C.J. and Cracknell, A.P., *The Mathematical Theory of Symmetry in Solids*, Clarendon Press, Oxford, 1972.

18. Jones, H., *The Theory of Brillouin Zones and Electronic States in Crystals*, North-Holland Publishing Co., Amsterdam, 1960.

19. Santamaria, F.G., "Photonic Crystals based on Silica Microspheres", Doctoral Dissertation, Instituto de Cinecia de Materiales de Madrid, 2003.

20. Andreani, L.C., Agio, M. and Botti, S., "Symmetry properties of two-dimensional photonic crystals", *Electrons and Photons in Solids*, Vol. 71, 2001.

Appendix I: Brillouin Zone for the Face-Centered Cubic Crystal Lattice

The face-centered cubic (FCC) crystal lattice is a classic Bravais lattice that forms the basis of the diamond structure. For completeness, a brief description of the FCC lattice is presented here. Naturally, there are three lattice vectors for the unit cell. In terms of the Cartesian unit vectors, these basis vectors are given as

$$\vec{a}_1 = \frac{a}{2}(\hat{j} + \hat{k}) \tag{6}$$

$$\vec{a}_2 = \frac{a}{2}(\hat{i} + \hat{k}) \tag{7}$$

$$\vec{a}_3 = \frac{a}{2}(\hat{i} + \hat{j}) \tag{8}$$

The lattice constant is denoted as "*a*", and the length of each lattice vector is $1/\sqrt{2}$ for a supercell consisting of the unit Cartesian cube. It is relatively easy to show that the basis vectors for the reciprocal lattice are:

$$\vec{b}_1 = \frac{2\pi}{a}(-\hat{i} + \hat{j} + \hat{k}) \tag{9}$$

$$\vec{b}_2 = \frac{2\pi}{a}(\hat{i} - \hat{j} + \hat{k}) \tag{10}$$

$$\vec{b}_3 = \frac{2\pi}{a}(\hat{i} + \hat{j} - \hat{k}) \tag{11}$$

Strangely enough, the reciprocal basis vectors are aligned with the lattice vectors for a body-centered cubic (BCC) crystal structure. The reciprocal basis allows the Brillouin zone to be defined. For the FCC lattice, the Brillouin zone is characterized as a truncated octahedron. A truncated octahedron is composed of two four-sided pyramids joined at the base and then truncated by cutting away all six corners. This Brillouin zone (BZ) is shown in Figure 23 along with its high symmetry points. In this case, the BZ has been augmented with additional symmetry points to help in bandgap studies. The basis symmetry points are: Γ - the BZ center, L - the center of a hexagonal face, X - the center of rectangular face, W – a corner, U – the center of a side adjoining hexahedral and square faces, K – the center of a side adjoining two hexahedral faces. In reciprocal space (k_x, k_y, k_z), these points have the coordinates listed below

$$\begin{aligned} \text{L} &= (\tfrac{1}{2}, \tfrac{1}{2}, \tfrac{1}{2}) \\ \text{W} &= (\tfrac{1}{4}, \tfrac{3}{4}, \tfrac{1}{2}) \\ \text{X} &= (0, \tfrac{1}{2}, \tfrac{1}{2}) \\ \text{U} &= (\tfrac{1}{4}, \tfrac{5}{8}, \tfrac{5}{8}) \\ \text{K} &= (\tfrac{3}{8}, \tfrac{3}{8}, \tfrac{3}{4}) \end{aligned} \tag{12}$$

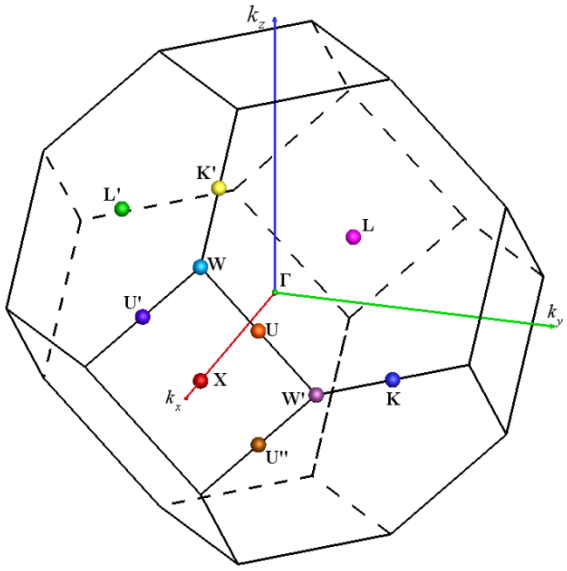

Figure 23. Brillouin zone for face-centered cubic lattices

Coordinates of these points in the Cartesian or physical lattice can be retrieved by using the transformation

$$(x, y, z) = \frac{a}{4\pi}(k_y + k_z, k_x + k_z, k_x + k_y) \tag{13}$$

With the careful use of vector algebra and Figure 23, the coordinates of all points (symmetry points and otherwise) comprising the BZ can be determined. It should be noted that the BZ axes need not be aligned in the manner show. In some cases, one may choose to align say, the k_z axis normal to a hexagonal face.

Appendix II: CTL File for the Diamond Minimal Surface

The ctl file for the diamond minimal surface required some effort and research time, so it is worthy of archiving. The mathematics of the minimal surface had to be translated into a series of Scheme expressions. These expressions had to work well with the rest of the MPB input syntax. For the crystal with volume fraction 0.19, the ctl file is provided below.

```
; diamond lattice - surface equation method test
; t = -0.756639 <=> phi = 0.19
;
(define pi 3.141592654)
(define a  1.0)
(define twopioa (/ (* 2 pi) a))
(define fr 0.0)
(define t -0.756639)
(define epsc 2.45)
(define epsa 1.0)
(define sx 0.0)
(define cx 0.0)
(define sy 0.0)
(define cy 0.0)
(define sz 0.0)
(define cz 0.0)

(define (px p) (vector3-x (lattice->cartesian p)))
(define (py p) (vector3-y (lattice->cartesian p)))
(define (pz p) (vector3-z (lattice->cartesian p)))

(define (eps-func p)
      (set! sx (sin (* twopioa (px p))))
      (set! cx (cos (* twopioa (px p))))
      (set! sy (sin (* twopioa (py p))))
      (set! cy (cos (* twopioa (py p))))
      (set! sz (sin (* twopioa (pz p))))
      (set! cz (cos (* twopioa (pz p))))
      (set! fr (+ (* cz (+ (* sx cy) (* cx sy)))
                  (* sz (+ (* cx cy) (* sx sy)))))
      (make dielectric (epsilon
                  (if (> fr t) epsa epsc ))))

(set! geometry-lattice (make lattice
    (basis-size (sqrt 0.5) (sqrt 0.5) (sqrt 0.5))
    (basis1 0 1 1)
    (basis2 1 0 1)
    (basis3 1 1 0)))
```

```
(set! k-points (interpolate 4 (list
    (vector3 0 0.5 0.5)              ; X
    (vector3 0 0.625 0.375)          ; U
    (vector3 0 0.5 0)                ; L
    (vector3 0 0 0)                  ; Gamma
    (vector3 0 0.5 0.5)              ; X
    (vector3 0.25 0.75 0.5)          ; W
    (vector3 0.375 0.75 0.375))))  ; K

(set! default-material (make material-function
        (material-func eps-func)))


(set-param! resolution 32)
(set-param! mesh-size 3)
(set-param! num-bands 3)

(run)
```

DISTRIBUTION LIST
AFRL-RW-EG-TR-2013-030

Defense Technical Information Center Attn: Acquisition (OCA) 8725 John J. Kingman Road, Ste 0944 Ft Belvoir, VA 22060-6218	1 Electronic Copy (1 file, 1 format)

EGLIN AFB OFFICES:

AFRL/RWOC (STINFO Tech Library Copy)	1 Copy
AFRL/RW CA-N	Notice of publication only